The Recognition and Control of Nonideal Soft-Switching Frequency for Wireless Power Transfer System Based on Waveform Identification

Yue Sun, *Member, IEEE*, Huan Zhang, Aiguo Patrick Hu, *Senior Member, IEEE*, Chun-Sen Tang, *Member, IEEE*, and Li-Juan Xiang

***Abstract*—Nonideal frequency problems can occur in a wireless power transfer system due to multiple soft-switching frequencies and frequency bifurcation. To make the system work at an ideal frequency with high-power transfer capability and efficiency, a method based on waveform identification is proposed. First, the space state model of a SP type WPT system is built, and the waveforms at ideal and nonideal working frequencies are obtained based on the stroboscopic mapping theory. Second, according to the characteristics of these waveforms, the swing door algorithm is improved by waveform distortion rate and fast Fourier transformation, which is used to recognize nonideal waveforms. Then, a control strategy based on "online self-determined optimization" is proposed to deal with the problem. Finally, the results of simulation and experiments show that the method proposed in this paper can identify the waveforms at nonideal frequency and find an ideal working frequency for the WPT system.**

***Index Terms*—Improved swing door algorithm (SDA), nonideal frequency recognition, online self-determined optimization, wireless power transfer (WPT).**

I. Introduction

WIRELESS power transfer (WPT) technology is mainly based on the principle of electromagnetic induction, transforming power from power supply to electrical equipment through air gap [1], [2]. It is safe, flexible, convenient, and artistic. Nowadays, WPT systems are widely used in electric vehicles' wireless charging, implantable biomedical equipment's wireless supplying, the rotating mechanism's wireless power supplying, tailless kitchen, mobile robots' wireless power supplying, etc. [3]–[6].

Manuscript received May 6, 2016; revised July 19, 2016; accepted August 17, 2016. Date of publication August 26, 2016; date of current version March 24, 2017. This work was supported in part by the research funds for the National High Technology Research and Development Program of China (863 Program) under Grant 2015AA016201 and in part by the Natural Science Foundation of China under Grant 61573074 and Grant 51277192. Recommended for publication by Associate Editor J. Acero.

Y. Sun is with the State Key Laboratory of Power Transmission Equipment and System Security and New Technology and College of Automation, Chongqing University, Chongqing 400030, China (e-mail: syue@cqu.edu.cn).

H. Zhang, C.-S. Tang, and L.-J. Xiang are with the College of Automation, Chongqing University, Chongqing 400030, China (e-mail: zh_seu@163.com; cstang@cqu.edu.cn; xianglijuan@cqu.edu.cn).

A. P. Hu is with the Department of Electrical and Computer Engineering, University of Auckland, Auckland 1142, New Zealand (e-mail: a.hu@auckland.ac.nz).

Color versions of one or more of the figures in this paper are available online at http://ieeexplore.ieee.org.

Digital Object Identifier 10.1109/TPEL.2016.2603531

Because a WPT system transmits power through the loose coupling magnetic field between coupling coils, compensation tank is usually used to make the system work at resonant state [7]. Thus, its power transfer capability and efficiency can be improved. However, this also makes it a high-order circuit system due to the storage elements exist in it [8]–[10]. A high-order circuit may have more than one soft-switching frequencies, but a soft-switching frequency is not always the resonant frequency, and not all the resonant frequencies make the system work well due to frequency bifurcation [11]. These frequencies are called nonideal frequencies in this paper. If a WPT system works at a nonideal frequency, the power transfer capability and efficiency of the system is low which makes the system cannot work normally. It may also cause some other problems such as high electromagnetic interference (EMI).

People have researched on the nonideal frequency problem of WPT systems. However, the existing literature mainly focus on frequency problem caused by illegal load and foreign subjects in the coupling mechanism [12]–[14]. Furthermore, the existing control methods are mainly concentrated on tuning by using capacitor array and controllable inductors [15], [16]. These two kinds of tuning methods work under hard-switching conditions, and cannot solve the nonideal frequency problem caused by multiple soft-switching frequencies and frequency bifurcation, either.

Therefore, it is meaningful to find a method to judge whether a WPT system works at a frequency which is not only soft-switching frequency, but also resonant frequency. Furthermore, at this resonant frequency, the system has high-power transfer capability and efficiency. We call it an ideal working frequency.

This paper proposed an improved swing door algorithm (SDA) to recognize the nonideal working frequency problem caused by multiple soft-switching frequencies and frequency bifurcation in a WPT system, and a control strategy based on "online self-determined optimization" is proposed to make the system work at an ideal frequency with high-power transfer capability and efficiency.

This paper is organized as follows. In Section II, a series-parallel (SP) type WPT system is taken to show the waveform characteristics at different soft-switching frequencies. In Section III, the traditional SDA is improved to recognize the nonideal frequency problem. In Section IV, the control method which can find an ideal frequency for the system is described.

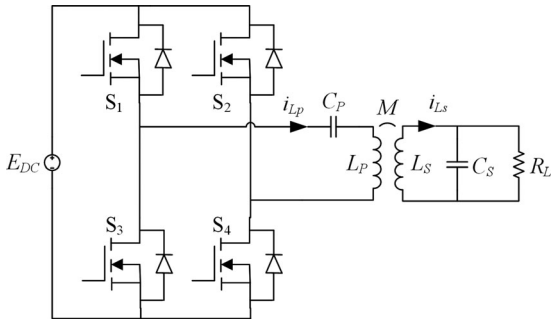

Fig. 1. Main circuit topology of a SP type WPT system.

The simulation and experimental results are shown in Section V, and conclusion of this paper is presented in Section VI.

II. Analysis of Waveforms at Different Frequencies in a WPT System

A. Topology of the Main Circuit

The waveforms at different soft-switching frequencies are different. To show the differences, a WPT system with SP type compensation structure is taken, and its circuit is shown in Fig. 1.

Considering the input source of the system is dc voltage, which will become square-wave voltage after high-frequency inverter. When the system is working at an ideal soft-switching point, the current in the primary coil has the same frequency with the square-wave voltage, and it should be standard sine waveform due to the filtering function of the resonant network. This current can satisfy the resonant frequency of primary and secondary side at the same time. So, the WPT system can transfer more power, and the efficiency is high. What's more, it can also decrease EMI, skin effect, and damage to the devices.

Taking use of ac impedance method to analyze the circuit in Fig. 1, and considering the fundamental component of the inverter voltage only, the system can work at resonant state on condition that the parameters are configured as

$$\begin{cases} C_S = \dfrac{1}{\omega^2 L_S} \\ C_P = \dfrac{L_S}{\omega^2 (L_P L_S - M^2)} \end{cases} \tag{1}$$

where ω is the working angular frequency of the system, and M is the mutual inductance.

According to this method, the parameters of the system are measured and configured, at 40 kHz, as follows: the inductance of primary energy transmitting coil $L_P = 28.68\ \mu$H, whose equivalent series resistance $r_P = 0.17\,\Omega$ and the compensating capacitor $C_P = 0.588\ \mu$F; the inductance of secondary energy pickup coil $L_S = 44.18\ \mu$H, whose equivalent series resistance $r_S = 0.19\ \Omega$ and the compensating capacitor $C_S = 0.358\ \mu$F; and the mutual inductance M between the two coils is 8.7 μH.

According to the analysis above, the soft-switching frequency of the system should be $f = \omega/2\pi = 40$ kHz. At this frequency point, the WPT system works well.

B. Stroboscopic Mapping Theory

In order to explore whether the actual frequency is consistent with the theory or not, the state-space model of the system is established as

$$\dot{x} = Ax + Bu = \begin{pmatrix} 0 & \dfrac{1}{C_P} & 0 & 0 \\ \dfrac{L_S}{\Delta} & \dfrac{L_S r_P}{\Delta} & \dfrac{M r_S}{\Delta} & \dfrac{M}{\Delta} \\ \dfrac{M}{\Delta} & \dfrac{M r_P}{\Delta} & \dfrac{L_P r_S}{\Delta} & \dfrac{L_P}{\Delta} \\ 0 & 0 & \dfrac{1}{C_S} & \dfrac{-1}{C_S R_L} \end{pmatrix} \begin{pmatrix} u_{C_P} \\ i_{L_P} \\ i_{L_S} \\ u_{C_S} \end{pmatrix} + \begin{pmatrix} 0 \\ \dfrac{-L_S}{\Delta} \\ \dfrac{-M}{\Delta} \\ 0 \end{pmatrix} u_{\text{in}} \tag{2}$$

In (2), x is the state vector of the system. It comes from the current flowing through the energy coils and the voltage of the compensating capacitors, respectively. The input of the system is $\pm E_{DC}$ in Fig. 1, which can be considered as linear within half a cycle. $\Delta = M^2 - L_P L_S$.

According to the stroboscopic mapping and periodic fixed point theory proposed in the literature [9], [10], the stroboscopic mapping model of nth steady period can be obtained as

$$x_{n+1} = f_{n+1}(f_n(x)) = e^{AT} x_n + \left(e^{\frac{AT}{2}} - I\right)^2 A^{-1} B E_{DC}. \tag{3}$$

When the system is steady, $x_{n+1} = x_n$. Making the period T a variable, so the periodic fixed point $x^*(t)$ can be represented as

$$x^*(t) = \left(I + e^{\frac{At}{2}}\right)^{-1} \left(I - e^{\frac{At}{2}}\right) A^{-1} B E_{DC}. \tag{4}$$

Because the current in the primary coil is needed, let the state selection matrix $Y = [0\ 1\ 0\ 0]$, so that the current can be obtained. The periodic fixed function $f(t)$ can be described as (5), where the nonzero solution of $f(t) = 0$ is the soft-switching cycle

$$f(t) = Y\left(I + e^{\frac{At}{2}}\right)^{-1} \left(I - e^{\frac{At}{2}}\right) A^{-1} B E_{DC}. \tag{5}$$

The analysis above does not take the parasitic and stray parameters into consideration, because their values are relatively too small at tens of kilohertz. The parasitic self-capacitances of the coils are much smaller than compensation capacitors'. As for equivalent series resistances of the coils, they get bigger when the frequency gets higher. However, they mainly bring in power loss, and make a little impact on the resonant frequency, according to (1). When a WPT system works at less than 1 MHz, the effect of these parameters can be ignored [17], and they do not put big influences on the control method below.

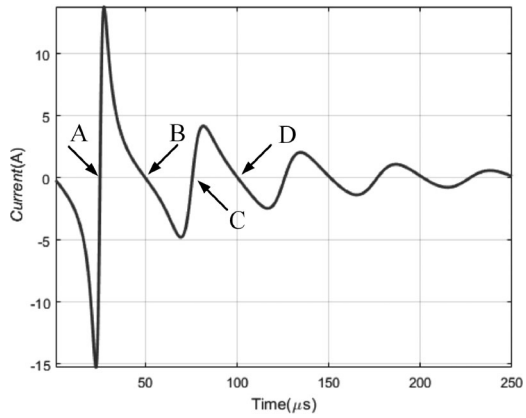

Fig. 2. Curve of the fixed point function.

C. Analysis of Soft-Switching Frequency Points

According to the analysis above, the periodic fixed function curve of the output current after the inverter bridge in SP type WPT system can be plotted as Fig. 2. At this time, the load resistor $R_L = 20\ \Omega$.

There are more than one soft-switching points in Fig. 2, only the former four points are taken to analyze, that is point A, point B, point C, and point D. The working period of these four points is 25.17, 49.88, 75.52, and 100.32 μs, and the corresponding working frequency is 39.73, 20.25, 13.24, and 9.97 kHz. Obviously, point A, 39.73 kHz is the ideal working frequency of the system, which is also the frequency by configuring parameters according to (1).

In order to observe the working status at the four soft-switching points, the voltage and current waveforms of the inverter at every point are drawn in Fig. 3.

In Fig. 3, the abscissa represents time, and ordinate represents the amplitude of inverting voltage $u_{\rm in}$ and current i_{Lp}. The square waveform with some distortion is inverting voltage $u_{\rm in}$, while the other waveform is inverting current i_{Lp}. They are also the voltage and current injected into the resonant network.

As shown in Fig. 3, the WPT system does work under soft-switching conditions at all of the four points. However, current waveforms at point B, point C, and point D distort seriously. Their frequencies deviate from the expected frequency and resonant frequency of the system. The effective value of the current is small too. So the system is unable to work normally. Only at point A, the system works at soft-switching state, the amplitude of the current is large, the frequency is consistent with the resonant frequency, and the waveform of current is quasi-sinusoidal. Therefore, point A is the ideal working frequency point of the system.

III. Method to Recognize Nonideal Frequency Problem

A. Theory of Basic SDA

According to the analysis in Section II, in a WPT system, there are more than one soft-switching frequencies due to the characteristics of a high-order circuit. When the system works at a nonideal soft-switching point, the total harmonic distortion is large which will make the devices heat seriously, the coupling mechanism damage, and some other issues. Furthermore, it will generate large EMI. The most serious problem is that the energy picked up by secondary side will decrease rapidly which may not satisfy the requirements of secondary side.

Only taking use of a simple soft-switching follower may make a WPT system work at a nonideal frequency. For such problems, judging whether the phase difference between input voltage $u_{\rm in}$ and current $i_{\rm in}$ is zero makes no sense. The working frequency of a WPT system is usually tens of kilohertz, and the current data in primary energy coil are numerous. Therefore, sampling data simply make it impossible to store such a huge amount of data, and it is likely to cause a great delay for the processing speed is too slow. Therefore, a recognition method based on improved SDA is proposed. The basic criterion is to judge whether the current flowing through the primary energy coil is quasi-sinusoidal and some other limiting conditions are added too.

The basic principle of the SDA is described below. SDA is a kind of fast algorithm for linear fitting [18], [19]. It is usually used to compress data in real-time database, and it makes the storage capacity greatly reduce. The basic idea is constructing many parallelograms with fixed height (height is the threshold of lossy compression) to "trap" data, and storing the former point when it cannot "trap" anymore. This algorithm is widely used in data compression and real-time storage of numerous data. Now, it is improved to recognize the nonideal frequency problem of WPT systems. The basic principle of SDA is shown in Fig. 4.

As shown in Fig. 4, SDA picks up the first point on vertical axis, sets threshold points above and below the first point, and the height of the threshold is $\Delta\varepsilon$. Now, assuming that there is a door beginning with the upper threshold point whose slope is negative infinity. Meanwhile, there is also a door beginning with the lower threshold point whose slope is positive infinity. That means the algorithm is at its initial state and the door is closed.

Now, taking point t_1 and connecting this point with two threshold points, as shown in Fig. 4. It can be seen that the absolute values of slope from point t_1 to threshold points are getting smaller. That means the slope of the two closed doors is changing and the doors are opening. After that points t_2 and t_3 are handled just like t_1. Until point t_4, the two doors are parallel. At this time, stop opening the door, store the starting and ending points, and begin a new round of algorithm.

B. Theory of Improved SDA

Traditional SDA mainly plays the role of data compressing, and it cannot be directly used to recognize the nonideal frequency problem in WPT systems. Therefore, three measures are proposed to improve it.

First, on basis of the results of traditional SDA, calculating the standard sine-wave function that should be approximated. The standard sine function is given as

$$y(t) = A\sin(\omega t + \varphi). \tag{6}$$

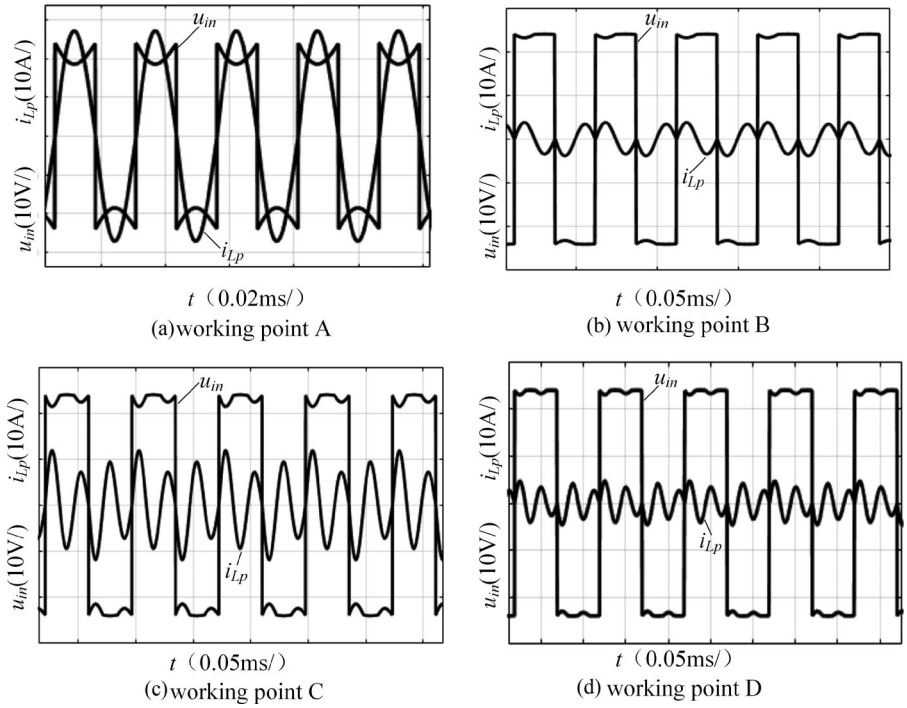

Fig. 3. Voltage and current waveforms of the inverter.

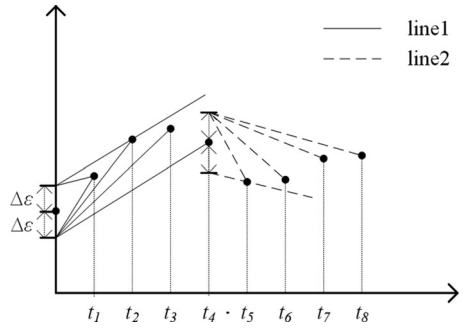

Fig. 4. Basic principle of a SDA.

In (6), there are three unknown variables. So, three points are needed to calculate its specific expression. It is useless to consider the phase of the sine wave in the proposed method, so phase variable φ is neglected. According to the analysis above, the standard sine wave has two zero-crossing points within a cycle, and their time difference is half cycle. So, the angular frequency ω can be determined. As for the amplitude, any other data can be used.

Second, the waveform distortion rate (WDR) is proposed. With its help, the degree of waveform distortion can be judged. Considering the actual circuit, the current in primary energy emission coil may not be absolutely standard sine wave. Therefore, by setting the margin of distortion rate, it is possible to allow slight distortion of the waveforms.

The basic idea of the recognition method is to judge whether the current waveform is quasi-sinusoidal, therefore, just defining the WDR simply as

$$\mu = \frac{1}{N}\sum_{i=1}^{N}\left(\left|\frac{y(x_i)-f(x_i)}{y(x_i)}\right|\right). \tag{7}$$

In (7), *y(x)* represents the standard sine-wave function, *f(x)* represents the data processed after SDA, and *N* is the total number of data remaining after processing. The basic idea is to determine the difference between actual current data and standard sine-wave function.

Finally, fast Fourier transformation (FFT) is taken after the processing of SDA. Taking use of total harmonics distortion (THD), that is the percentage of fundamental wave and high-order harmonics to judge whether the waveform is normal or not.

Adding these limits into traditional SDA, setting the WDR μ, and threshold of THD properly to determine whether the nonideal frequency problem exists in the system.

C. Identify the Waveforms by Improved SDA

According to the improvement measures mentioned above, the current waveforms in Fig. 3 are extracted separately, and the improved SDA is used to process it. The waveforms after identification are shown in Fig. 5.

Fig. 5(a)–(d) shows the primary resonant current i_{Lp} at the four soft-switching points. The solid line is the actual current waveform. That is the original data processed by improved SDA. The symbol "$*$" on the solid line represents the output of traditional SDA. The dotted line is the standard sine wave getting from improved SDA.

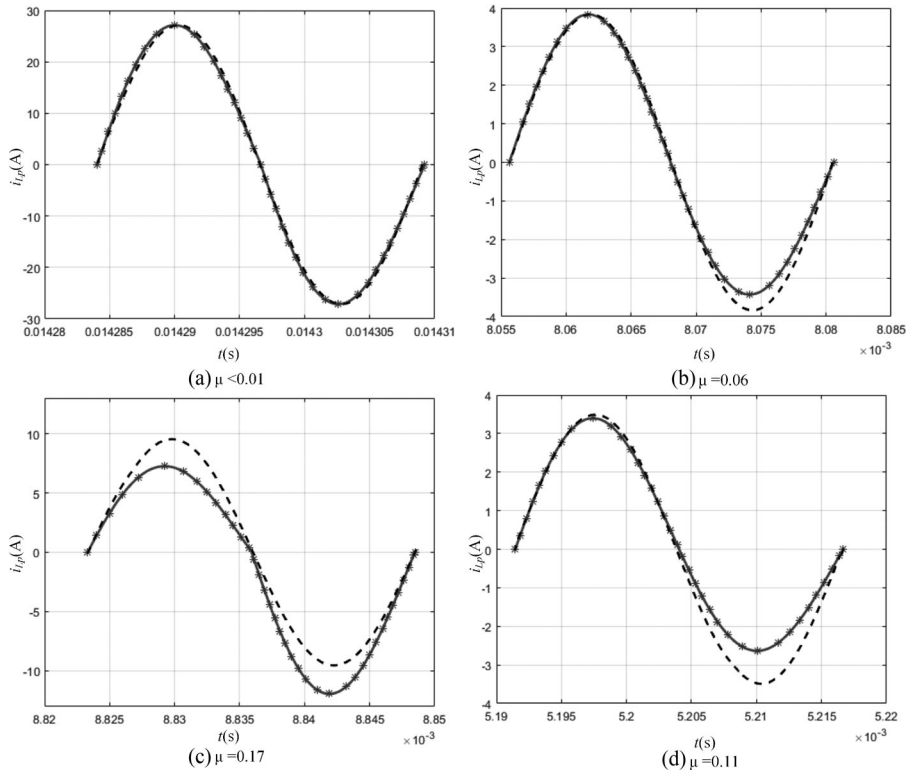

Fig. 5. Results of the improved SDA.

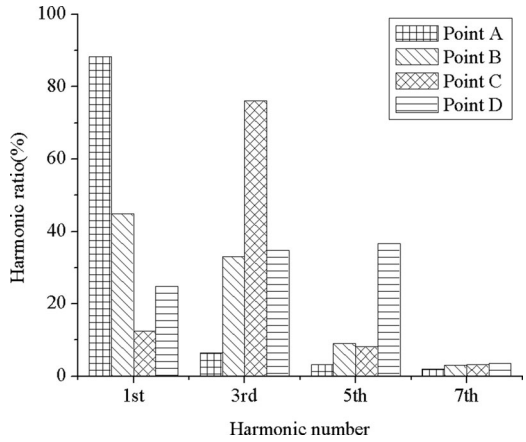

Fig. 6. Harmonic analysis of the system.

From the comparison of Figs. 3 and 5, it can be seen that considering each small current cycle, the waveforms are very likely to standard sine wave when seeing with naked eyes. However, by using the proposed method to recognize the waveform, as can be seen, the WDR of Fig. 5(a) is extremely low, while the WDR of Fig. 5(b)–(d) is relatively high. Furthermore, compared with standard sine wave, the difference is obvious.

In order to highlight the distortion of waveforms at the four frequencies, the data of current waveforms are processed by FFT. The results are shown in Fig. 6, where the abscissa represents *n*th harmonic at different frequencies, and ordinate represents their percentage among all the harmonics.

According to Figs. 5 and 6, both "WDR" and "THD" can be separately used as a judgement to determine whether the waveform is standard sine. However, they are used together in this paper, because "WDR" takes less time and is easy to realize, "THD" of different waveforms has a big difference, while it takes more time to operate compared with "WDR." Therefore, "WDR" is used to save time, and "THD" is used to improve accuracy.

IV. Control Method

According to the previous description, a WPT system should satisfy several conditions at the same time if it works normally. First, current flowing through the energy emission coil should be quasi-sinusoidal. Second, the frequency of this sinusoidal current should be identical with the inverter voltage. Third, the phase difference of the sinusoidal current and inverter voltage should be zero. Finally, if the parameters are configured correctly, the frequency will not be too different from the setting frequency under normal circumstances.

Therefore, the control target in this paper is to find a frequency which can satisfy all the conditions above. When it satisfies the conditions, the WPT system operates well. The primary and secondary sides are all working at resonant state. That is good for the power transferring while the EMI, skin effect, and damage to the devices are limited.

Considering the needs above, a method based on "online self-determined optimization" is proposed to control the nonideal frequency problem. The core idea is to make the working

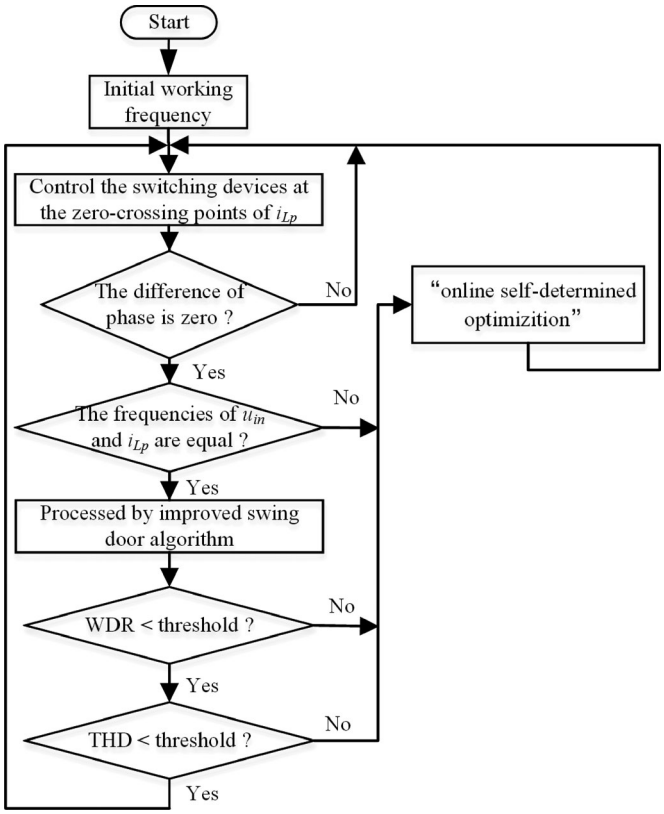

Fig. 7. Flowchart of the system.

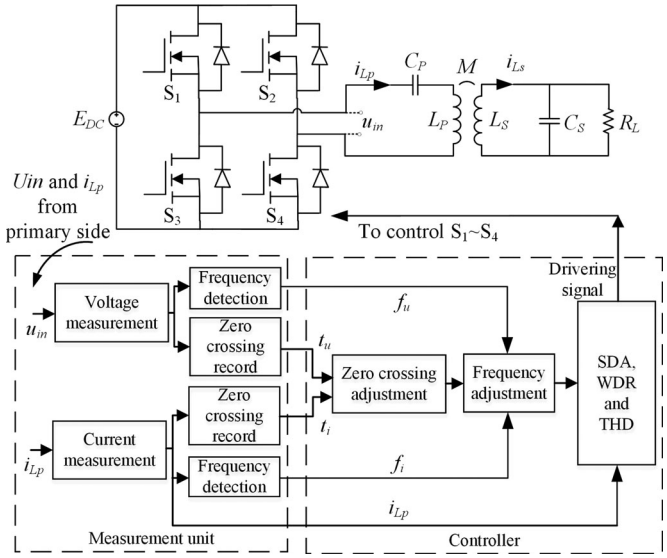

Fig. 8. Schematic diagram of the system with control.

frequency of the system varies within a certain range. At the same time, taking use of improved SDA to identify the waveforms. When the identified waveform satisfies all of the above requirements, it means the ideal working frequency is found. The control flowchart of the system is shown in Fig. 7.

The control method works at the basis of soft switching, so the beginning step is to find a soft-switching frequency. There are mainly four judgment conditions in Fig. 7. The first one is to judge whether the working frequency is a soft-switching frequency, the second one is to judge whether the soft-switching frequency is a resonant frequency, while the other two are used to determine whether the resonant frequency is an ideal frequency.

Now, the working principle of control logic will be discussed carefully. First of all, the system has an initial frequency, and works at hard-switching state. Then, it starts to follow the zero-crossing points of inverter current until the phase difference of inverter current and voltage is zero.

That means a soft-switching frequency is found. So, the next step is to judge whether this soft-switching frequency is also a resonant frequency of the system. If it is, the recognition program will identify the waveforms of inverter current, and judge whether this resonant frequency is an ideal frequency according to WDR and THD. If all the conditions are satisfied, the system is working at an ideal frequency.

If a soft-switching frequency cannot meet all of the above conditions, the system gets into control program of nonideal frequency problem. That is, "online self-determined optimization" state.

In this state, the working frequency of the system is changing from current frequency until it reaches to the threshold. The direction will be determined by the phase between inverter current and voltage. If a soft-switching point is met, the program starts to recognize again.

If none of the frequencies are soft-switching frequencies, they are not the resonant frequencies either. So the system will ignore them directly and change the direction.

If no frequency point is found in the process above, it means there is serious fault in the system. Maybe the compensating capacitor or the inductance of the coupling coil has changed seriously. Anyway, the WPT system cannot solve the problem itself, and needs manual help.

At the whole recognition and control process, the working frequency of the system will change only when the judgment is clear. If not, the system will keep working in soft-switching state. The recognition part is always running even the ideal frequency is found, because the ideal frequency may change when the system is subject to interference. Of course, if there is no interference, the control part does not response.

According to the control method above, the schematic diagram of the WPT system can be drawn as Fig. 8. As can be seen, the upper part is main circuit, and the lower shows the measurement unit and controller. According to the recognition method in Section III, the lower part takes use of the inverter voltage and current to judge the working state of the system, and then outputs the driving signal based on the control method in this section.

The fault discussed above is caused by the characteristics of a high-order circuit, and without external interference. Actually, there are some other factors that may affect the system, such as the change of load resistance. This can bring the problem of bifurcation, and will be described below.

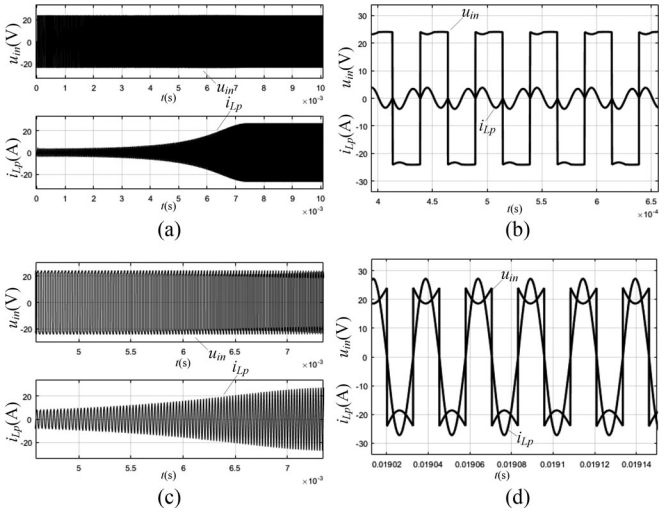

Fig. 9. Simulation waveforms of the control process.

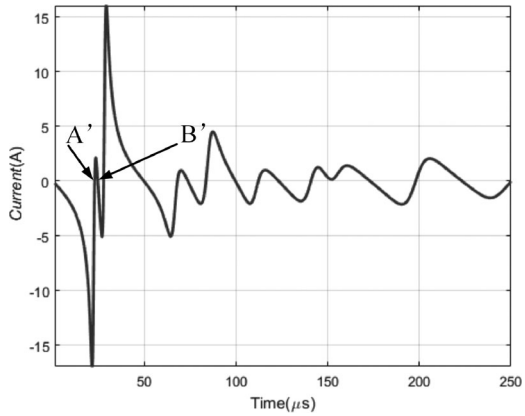

Fig. 10. Curve of the fixed point function.

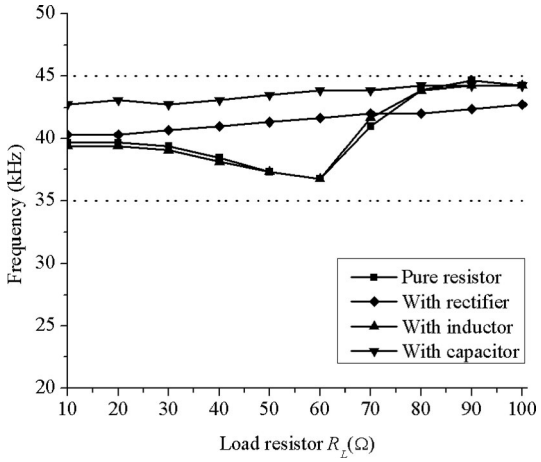

Fig. 11. Ideal frequency when the load changes with the control method.

V. Simulation and Experimental Study

In this paper, a nonideal frequency problem in WPT systems is described. To recognize and solve the problem, improved SDA and control method based on "self-determined optimization" are proposed. In order to prove the methods, the simulation model and experimental platform are built according to Figs. 1, 7, and 8.

A. Simulation Study

The simulation model is built under MATLAB/Simulink, according to Figs. 1, 7, and 8. The input dc voltage is 24 V, the load resistance is 20 Ω, and other parameters are shown in the end of Section II-A.

The key part is the control part, which consists of several functions. The inputs of these functions are the data of inverter current and voltage. According to the process in Figs. 7 and 8, these data are judged and processed. Based on the results, the controller outputs driving signal with different frequency, and find an ideal one to make the WPT system work well.

Fig. 9 is the results of simulation. It shows the control waveforms based on "online self-determined optimization". Fig. 9(a) is the waveforms of the entire control process. Fig. 9(b) is the local amplification when the control begins. Fig. 9(c) is the local amplification of "online self-determined optimization". Fig. 9(d) is the local amplification of steady state when the control ends.

As can be seen, the WPT system works at nonideal soft-switching frequency at first. When the control method starts working, the frequency of the system is changed gradually, and the ideal soft-switching frequency is found finally. So, the control of the nonideal frequency problem is realized.

The recognition of simulation waveforms has been given in Figs. 5, 6, and 9. Some readers may think the four frequency points in Fig. 2 have significant difference. They can be distinguished just by frequency limits. To solve this doubt, we use the SP type WPT system and the parameters in this paper, and just change the resistance of load from 20 to 80 Ω. The periodic fixed point function is shown in Fig. 10.

As can be seen, the former two points are closed to each other, and they are both resonant frequencies, i.e., frequency bifurcation. If we only rely on frequency restriction, it is impossible to recognize or control this kind of problem. Therefore, it is necessary to find a new method to solve this problem. The recognition waveforms of Fig. 10 can be obtained according to the method proposed in this paper. We do not repeat them due to the space limitations. The former two points A′ and B′ in Fig. 10 are taken as an example, whose frequencies are 43.92 and 40.79 kHz, respectively. For the space limits, the control waveforms will be given in experimental part directly, and the simulation waveforms are omitted.

The theoretical analysis section above mainly considers the load as purely resistive. To verify the validity of the control method, the load is set under four different conditions, and the control results are shown in Fig. 11. The first is pure resistor R_L, the second is R_L with a rectifier bridge, the third is R_L series with an inductor $L_L = 10$ μH, and the last is R_L series with a capacitor $C_L = 0.1$ μF.

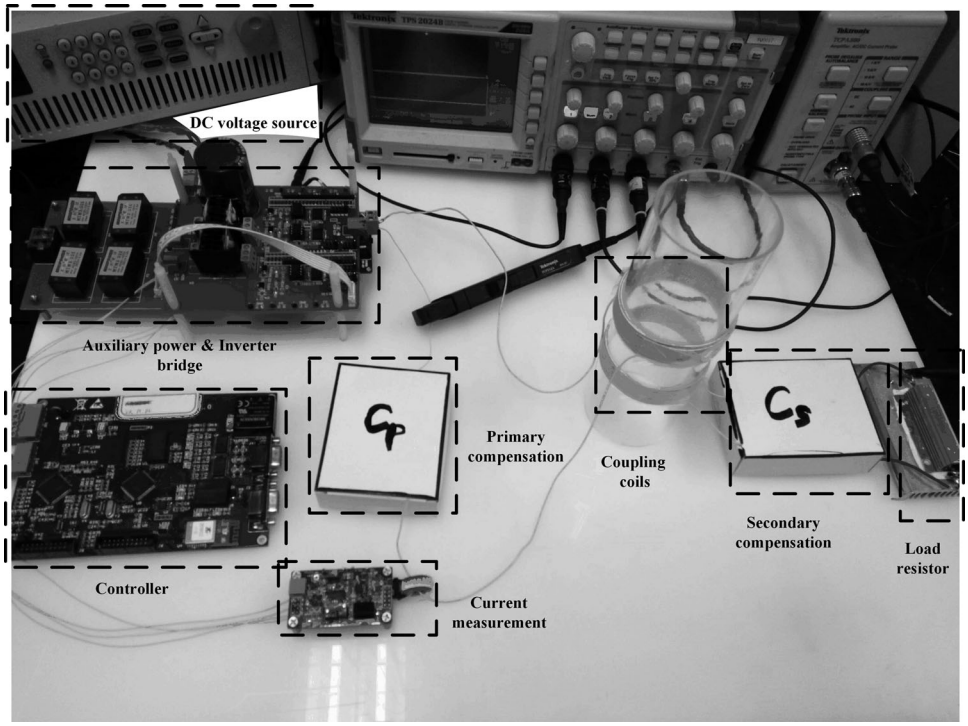

Fig. 12. Experimental platform.

In Fig. 11, the horizontal axis shows the numerical values of the load resistor resistance R_L, and the vertical axis shows the ideal working frequency. As can be seen, if the influences caused by the reactive or nonlinear parts are limited, the working frequency would not go beyond the searching threshold of the algorithm, and the proposed control method can always find the ideal frequency. However, if the influences are great, the working frequency will go beyond the searching threshold, and the system cannot work normally with present parameters. At this time, the compensation network should be changed to make the resonant frequency close to the design one (40 kHz in this paper), and then the control method can be taken to find the specific value of the ideal frequency. The influences of different loads can be found in the literature [20], [21]. The threshold of frequency is set based on the practical requirements. For example, we can set 40 ± 5 kHz in Fig. 11.

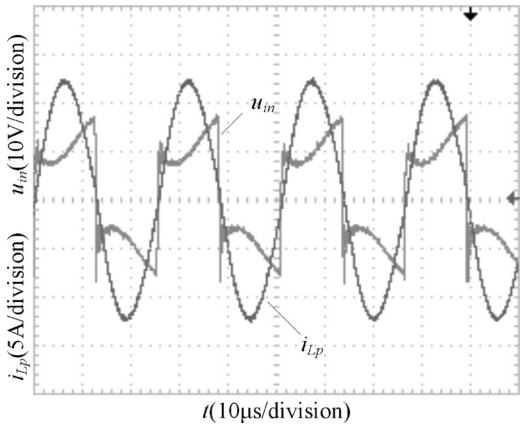

Fig. 13. Waveforms of ideal soft-switching frequency A.

B. Experimental Study

The experimental platform is built and shown in Fig. 12, aims to realize the recognition and control of nonideal frequency problem in a WPT system. The input dc voltage is 12 V, the load resistance is 20 Ω, and other parameters are shown in Section II-A. The main control chip in Fig. 12 is STM32F765IG, and the transistors are STP30NF20.

As can be seen, there are eight parts in Fig. 12, 1) the dc voltage source; 2) the auxiliary power and inverter bridge; 3) the primary compensation; 4) the coupling coils; 5) the secondary compensation; 6) the load resistor; 7) the measurement; 8) and the controller. The experimental waveforms are all tested on this practical circuit.

To verify the method proposed in this paper, Figs. 13–Fig. 15 are given below. In these figures, $u_{\rm in}$ is the output voltage of inverter, i_{Lp} is the output current of inverter, which is also the current in the primary coil. Fig. 13 shows the waveforms when the system is working at an ideal frequency, while Fig. 14 is working at a nonideal frequency. Fig. 15 is the recognition and control process when the nonideal frequency problem appears.

As can be seen, when the system works well, the current is quasi-sinusoidal and the magnitude is high. On the contrast, when it works at a nonideal frequency, the waveforms distort seriously, and the magnitude is very low, which cannot meet the requests of the system. When the nonideal frequency problem

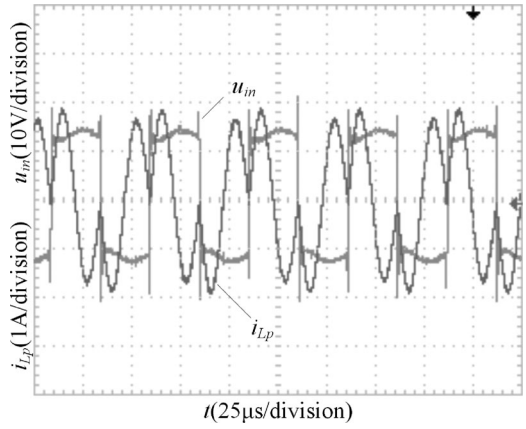

Fig. 14. Waveforms of nonideal soft-switching frequency B.

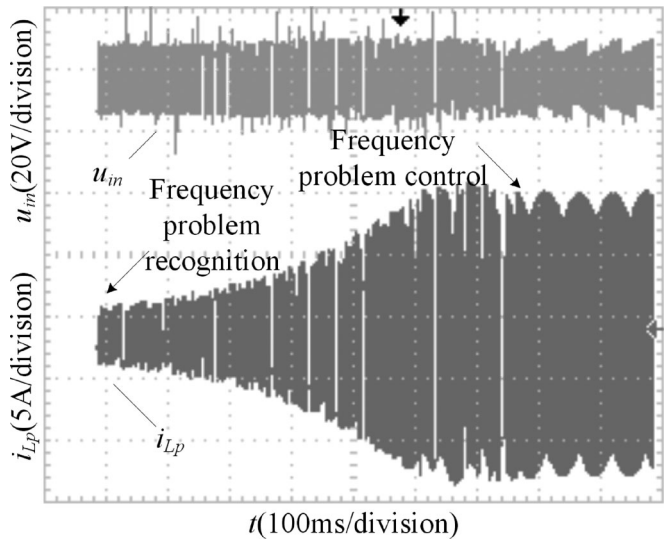

Fig. 15. Process of problem control.

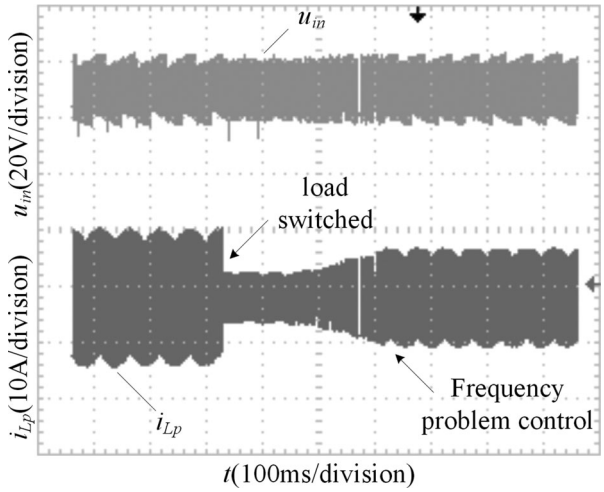

Fig. 16. Process of problem control after load switched.

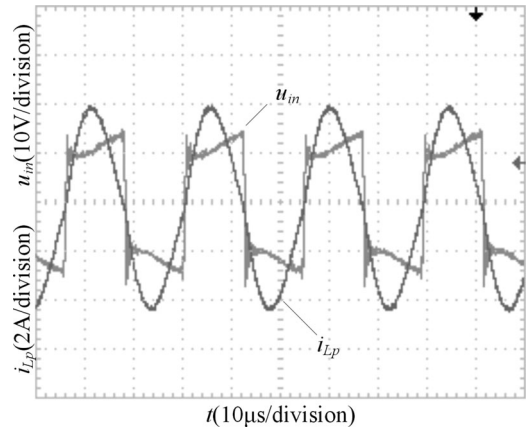

Fig. 17. Nonideal frequency waveform after load switched.

occurs, the recognition program can pick it up and the control program takes action very quickly. So the problem can be solved.

As can be seen, the waveforms of the inverter voltage in Figs. 13 –15 are depressed, also in some other experimental and simulation figures. That is mainly caused by the characteristics of the system, whose voltage is low, while the current is high. Therefore, the inner resistor of the dc voltage source and the on-state resistor of the switching devices make some impacts. When the transient value of the inverter current i_{Lp} gets higher, the voltage lost on them increases too.

There are some spikes in Fig. 14, they are caused by the nonideal characteristics of detection and switching devices, and the ZVS state is not 100%. Actually, it is difficult to make the spikes disappear, but the spikes can be greatly suppressed.

As for the amplitude fluctuation in lower frequency in Fig. 15, it is caused by the characteristics of oscilloscope, and the system itself is stable.

In order to verify the frequency bifurcation problem proposed in the beginning of this section, Fig. 16 is given above. It is the control process when the load is changed, and, thus, the resonant frequency is changed. As can be seen, under this condition, the recognition and control program can solve this problem too.

To make it clearly, the waveforms at nonideal and ideal soft-switching frequencies after the load switched are given below. Fig. 17 shows the nonideal soft-switching frequency waveforms, while Fig. 18 shows the ideal. The working frequency in Fig. 17 is 40.79 kHz (at point B′), and it is 43.92 kHz (at point A′) in Fig. 18.

Readers may think the current waveforms in Figs. 17 and 18 are both good sine, so the proposed method cannot work. Actually, it can be seen that the current waveform in Fig. 17 is vertically asymmetric, and it is distorted at the switching points. Therefore, THD in Fig. 17 is beyond the threshold, and the control method can distinguish it. One more kind of situation is that A' and B' in Fig. 10 are very close to each other. At this time, the two frequencies are both ideal and stable, their "WDR" and "THD" are both within the threshold, and the system can work well at each one of them [9], [10].

Fig. 19 shows the power transfer efficiency versus load resistor with and without the proposed control method, the input voltage remain 12 V, while the load resistor changes from 10 to

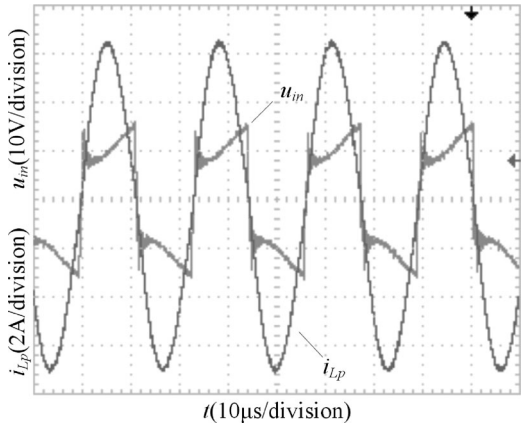

Fig. 18. Ideal frequency waveform after load switched.

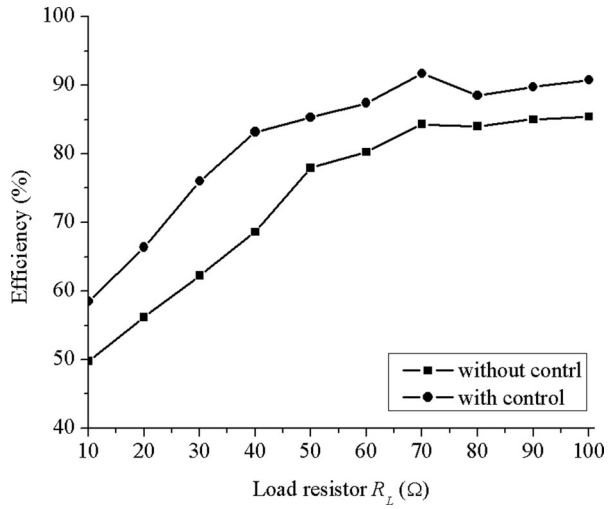

Fig. 19. Efficiency versus load with and without the proposed control method.

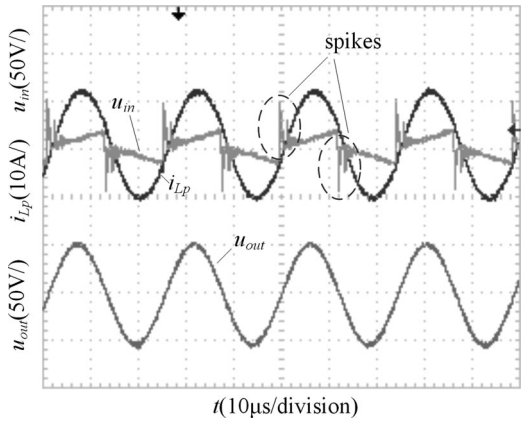

Fig. 20. Waveforms without the proposed control method.

100 Ω. As can be seen, the efficiency of the WPT system gets higher when R_L gets bigger. After the control method is taken, the maximum efficiency improvement can reach to 14.4%, when R_L is 40 Ω. That proved the advantage of the control method.

Fig. 20 shows the waveforms without the control method. Its experimental condition is the same as Fig. 13, while the only difference is that the control method is taken in Fig. 13. As can be seen, if there is no control method, lots of spikes appear when the switching devices turn on and off. However, in Fig. 13, the spikes are much fewer. According to Fig. 6, the ratio of harmonics in Fig. 13 is much lower than that in Fig. 14, and the quality of waveforms with control is much better than that without control. All in all, when the control method is taken, the harmonics and spikes are greatly depressed. Therefore, conducted and radiated EMI can be reduced too.

VI. Conclusion

This paper proposed a novel method based on waveform identification to recognize and control the nonideal soft-switching frequency problem in WPT systems. This problem is caused by multiple soft-switching frequencies and frequency bifurcation. First of all, the state-space model of a SP type WPT system is established, and the waveforms at different soft-switching frequencies are given based on stroboscopic mapping and periodic fixed point theory. Then, the traditional SDA is improved mainly by WDR and FFT to recognize whether there is a nonideal frequency problem in the system. After that the control method based on "self-determined optimization" is proposed to make the system works at an ideal frequency. Its basic idea is to change the frequency within the threshold and find one that can make the system works well. Finally, the methods are verified by MATLAB/Simulink simulation and practical experiments.

The proposed methods can be used to recognize the nonideal soft-switching frequency problem of the WPT system, and make the system works at an ideal frequency.

Reference

[1] S. Y. R. Hui, W. Zhong, and C. K. Lee, "A critical review of recent progress in mid-range wireless power transfer," *IEEE Trans. Power Electron.*, vol. 29, no. 9, pp. 4500–4511, Apr. 2014.

[2] S. D. Barman, A. W. Reza, N. Kumar, M. E. Karim, and A. B. Munir, "Wireless powering by magnetic resonant coupling: Recent trends in wireless power transfer system and its applications," *Renew. Sustainable Energy Rev.*, vol. 51, pp. 1525–1552, Jul. 2015.

[3] Z. Wang, X. Wei, and H. Dai, "Design and control of a 3 kW wireless power transfer system for electric vehicles," *Energies*, vol. 9, no. 1, pp. 1–10, 2016.

[4] X. Li, X. Meng, C. Tsui, and W. Ki, "Reconfigurable resonant regulating rectifier with primary equalization for extended coupling- and loading-range in bio-implant wireless power transfer," *IEEE Trans. Biomed. Circuits Syst.*, vol. 9, no. 6, pp. 875–885, Dec. 2015.

[5] M. Sato, G. Yamamoto, D. Gunji, T. Imura, and H. Fujimoto, "Development of wireless in-wheel motor using magnetic resonance coupling," *IEEE Trans. Power Electron.*, vol. 31, no. 7, pp. 5270–5279, Jul. 2015.

[6] D. Kim, M. Kim, J. Yoo, H. H. Park, and S. Ahn, "Magnetic resonant wireless power transfer for propulsion of implantable micro-robot," *J. Appl. Phys.*, vol. 117, no. 17, p. 17E712-1–17E712-4, May 2015.

[7] C. Yang and K. Tsunekawa, "Analysis and performance improvement of independent electric coupled resonance WPT system with impedance transformer," *IEICE Trans. Commun.*, vol. E98B, no. 4, pp. 630–637, Apr. 2015.

[8] M. Iordache, L. Mandache, D. Niculae, and L. Iordache, "On exact circuit analysis of frequency splitting and bifurcation phenomena in wireless power transfer systems," in *Proc. Int. Symp. Signals, Circuits Syst. Conf.*, 2015, pp. 1–4.

[9] Y. Sun, C. Tang, A. P. Hu, H. L. Li, and S. K. Nguang, "Multiple soft-switching operating points-based power flow control of contactless power transfer systems," *IET Power Electron.*, vol. 4, no. 6, pp. 725–731, Jul. 2011.

[10] C. Sen Tang, Y. Sun, Y. G. Su, S. K. Nguang, and A. P. Hu, "Determining multiple steady-state ZCS operating points of a switch-mode contactless power transfer system," *IEEE Trans. Power Electron.*, vol. 24, no. 2, pp. 416–425, Feb. 2009.
[11] B. Wang, H. A. Hu, and B. David, "Maintaining middle zero voltage switching operation of parallel-parallel tuned wireless power transfer system under bifurcation," *IET Power Elecron.*, vol. 7, no. 1, pp. 78–84, 2014.
[12] Z. N. Low, J. J. Casanova, P. H. Maier, J. A. Taylor, R. A. Chinga, and J. Lin, "Method of load/fault detection for loosely coupled planar wireless power transfer system with power delivery tracking," *IEEE Trans. Ind. Electron.*, vol. 57, no. 4, pp. 1478–1486, Apr. 2010.
[13] S. Fukuda, H. Nakano, Y. Murayama, T. Murakami, O. Kozakai, and K. Fujimaki, "A novel metal detector using the quality factor of the secondary coil for wireless power transfer systems," in *Proc. IEEE Int. Microw. Workshop Series Innov. Wireless Power Transm., Technol., Syst., Appl. Conf.*, 2012, pp. 241–244.
[14] Y. Su, H. Zhang, Z. Wang, A. Patrick Hu, L. Chen, and Y. Sun, "Steady-state load identification method of inductive power transfer system based on switching capacitors," *IEEE Trans. Power Electron.*, vol. 30, no. 11, pp. 6349–6355, Nov. 2015.
[15] H. Qiang, X. Huang, L. Tan, Q. Ji, and J. Zhao, "Achieving maximum power transfer of inductively coupled wireless power transfer system based on dynamic tuning control," *Sci. China Technol. Sci.*, vol. 55, no. 7, pp. 1886–1893, Jul. 2012.
[16] Y. Jiang, H. Zhou, W. Hu, and X. Gao, "Optimal parameter matching based on capacitor array for magnetically-resonant wireless power transfer system," *Dianli Zidonghua Shebei/Electr. Power Autom. Equip.*, vol. 35, no. 11, pp. 129—136, Nov. 2015.
[17] Q. Ke, W. J. Luo, G. Z. Yan, and K. Yang, "Analytical model and optimized design of power transmitting coil for inductively coupled endoscope robot," *IEEE Trans. Biomed. Eng.*, vol. 63, no. 4, pp. 694–706, Apr.
2016.
[18] M. Cui, J. Zhang, A. R. Florita, B. Hodge, D. Ke, and Y. Sun, "An optimized swinging door algorithm for identifying wind ramping events," *IEEE Trans. Sustainable Energy*, vol. 7, no. 1, pp. 150–162, Jan.2016.
[19] Y. V. Makarov, C. Loutan, J. Ma, and P. de Mello, "Operational impacts of wind generation on California power systems," *IEEE Trans. Power Syst.*, vol. 24, no. 2, pp. 1039–1050, May 2009.
[20] M. Xue, Q. X. Yang, Y. Li, X. Zhang, and W. N. Liu, "The study of load characteristic in wireless energy transfer system based on EM coupling resonance," *Trans. China Electrotechn. Soc.*, vol. 28, no. Suppl. 2, pp. 28–34, 2013.
[21] M. P. Theodoridis, "Effective capacitive power transfer," *IEEE Trans. Power Electron.*, vol. 27, no. 12, pp. 4906–4913, Dec. 2012.

Yue Sun (M'07) received the B.E. degree in electrical engineering, the M.E. degree in industry automation, and the Ph.D. degree in mechanical electrical integrated manufacturing from Chongqing University, Chongqing, China, in 1982, 1988, and 1995, respectively.

In 1997, he was a Senior Visiting Scholar in France for one year. From 2008 to 2009, he was a Visiting Scholar with the University of Queensland, Brisbane, Australia. He is currently a Professor with the State Key Laboratory of Power Transmission Equipment and System Security and New Technology and the College of Automation, Chongqing University. His research interests include automatic control, wireless power transfer, power electronics applications, and control theory and applications.

Huan Zhang received the B.E. degree from the College of Automation, Southeast University, Nanjing, China, in 2014. He is currently working toward the M.E. degree in control science and engineering in the College of Automation, Chongqing University, Chongqing, China.

His current research interests include wireless power transfer technology, power electronics, and control theory.

Aiguo Patrick Hu (M'01–SM'07) received the B.E. and M.E. degrees from Xian JiaoTong University, Xian, China, in 1985 and 1988, respectively, and the Ph.D. degree from the University of Auckland, Auckland, New Zealand, in 2001,

He was a Lecturer, a Director of China Italy Cooperative Technical Training Center, Xian, and the General Manager of a technical development company. Funded by Asian2000 Foundation, he was with the National University of Singapore for a semester as an exchange Postdoctoral Research Fellow. He is currently in the Department of Electrical and Computer Engineering, University of Auckland, and also the Head of Research of PowerbyProxi, Ltd. He holds 15 patents in wireless/contactless power transfer and microcomputer control technologies, published more than 200 peer-reviewed journal and conference papers, authored a monograph on wireless inductive power transfer technology, and contributed four book chapters.

Chun-Sen Tang (S'08–M'09) received the B.E. and Ph.D. degrees from the College of Automation, Chongqing University, Chongqing, China, in 2004 and 2009, respectively.

In 2008, he was a Research Fellow in the Department of Electrical and Computer Engineering, The University of Auckland, Auckland, New Zealand. In 2009, he joined the College of Automation, Chongqing University, where he is currently an Associate Professor. His current research interests include nonlinear modeling and analysis, intelligent control, and wireless power transfer.

Li-Juan Xiang received the B.E. degree from the College of Automation, Chongqing University, Chongqing, China, in 2012, where she is currently working toward the Ph.D. degree in the control theory and control engineering.

Her current research interests include wireless power transfer technology, power electronics, and optimization algorithms.